

Blade Mistuning Induced Blisk Vibration

T. Klauke, A. Kühhorn, B. Beirow

BTU Cottbus, Chair of Structural Mechanics and Vehicle Vibrational Technology,
Siemens-Halske-Ring 14, 03046 Cottbus,
Germany

OVERVIEW

Variations of blade-geometry or -material in bladed structures like compressor rotors result in localized vibration modes, higher displacement amplitudes, critical stress levels and reduced high cycle fatigue strength (*HCF-strength*) of several blades due to inauspicious aerodynamic excitations.

Based on numerical investigations an overview of the vibrational behavior in particular of mistuned blisks is presented in detail. Localized vibration modes are evaluated using a new criterion and illustrated in detail for updated full finite element models of the first rotor stages¹ from the *Engine 3E*² research program high pressure compressor (*HPC*) (see FIG. 1).

The investigations show, that in general the blade mode, the blisk geometry, especially the disk stiffness, are major factors for the level of mode localization. Due to the higher share of blades on the whole blisk strain energy, blade torsion modes of blisks with higher disk stiffness have a significant higher sensitivity to mistuning than blade bending modes of blisks with lower disk stiffness.

In this context it can be also concluded, that modified cyclic symmetry modes (*MCSM*), which are arisen out of cyclic symmetry modes (*CSM*) with lower numbers of nodal diameters, are less sensitive regarding blade mistuning compared to modes, which are arisen out of *CSMs* with higher numbers of nodal diameters.

An understanding of these coherences is a step towards to reduction of mistuning caused effects for future aero engines and also the base for the improvement of strain gauge instrumentation of mistuned bladed integrated disks.

NOMENCLATURE

<i>CSM</i>	= cyclic symmetry mode (number of circulating sine waves of a vibration mode, number of nodal diameters of a vibration mode resp.)
<i>CSM_{max}</i>	= highest cyclic symmetry mode
<i>D</i>	= dimensionless damping value
<i>DFT</i>	= coefficient of Fourier transformation
<i>E</i>	= Young's modulus [N/mm ²]
<i>EO</i>	= engine order
<i>f</i>	= frequency [Hz]
<i>f_n</i>	= eigenfrequency of blade <i>n</i> [Hz]
\bar{f}	= mean value of all blade eigenfrequencies [Hz]
<i>FRF</i>	= frequency response function
<i>HCF</i>	= high cycle fatigue
<i>HPC</i>	= high pressure compressor
<i>IBR</i>	= integrated bladed rotor, blisk
<i>i</i>	= component of displacement vector, blade number resp.

<i>LocaFac</i>	= localization factor of a vibration mode
<i>N</i>	= number of blades of a blisk
<i>ND</i>	= nodal diameter
<i>Q</i>	= quality factor, $Q = 1/2D$
<i>RMS</i>	= root mean square
<i>s/g</i>	= strain gauge
<i>t</i>	= time [s]
<i>U</i>	= displacement vector
ζ	= maximum blade displacement / root mean square
φ_{CSM}	= blade phase angle [rad]
ω	= eigenfrequency, $\omega = 2\pi f$



FIG 1. *Engine-3E-I-HPC* blisk stage 1 and 6

1. INTRODUCTION

Aiming at more environmental-friendly, more efficient and more powerful aero engines, integrated bladed disks (blisks³) become more important in the further development of aero engines (Steffens [2000, 2001]).

The vibrational behavior of conventional bladed disk assemblies was investigated in detail a long time before (for example Campbell [1924], Malkin [1942], Armstrong [1955], Kirkhope [1971] and Soares [1976]). In contrast to these assemblies the deletion of the heavy blade-disk connection results in reduced masses, higher maximum rotational velocities and improved pressure ratios (increased efficiency factors).

In this connection a number of disadvantages occur as very low structural damping and higher sensitivity with regard to manufacturing- and material tolerances (mistuning) [Beirow 2005].

Especially the negative effects of mistuned bladed disks have been studied longer than thirty years. Ewins [1969, 1973] showed that blade-to-blade deviations occur in higher blade displacement amplitudes in combination with a splitting of double modes. Whitehead [1966, 1998] derived a

1. 25 blades, 29 blades resp., titanium alloy
2. german research program aiming at new HPC technologies, 3E = efficiency, economy, ecology

3. or integrated bladed rotor, *IBR*

maximum amplitude magnification factor which predicts the increased maximum forced vibration response of blades due to mistuning.

Pierre and Wei [1987a, 1987b] considered that the mistuned case represents perturbations of the tuned system. They conclude that the vibrational behavior depends on the ratio of absolute amount of mistuning strength and the coupling between the blades through the disk. In addition, Griffin and Hoosac [1984] and Bladh [2003] determined the influence of inter-blade coupling on localized blade modes. Kielb and Kaza [1984], Wildheim [1979], Wilson [1993] determined unsteady blade loads arising from the fluctuating forces due to passing of wake shedding through the blade rows. The aerodynamic coupling of the blades was included in the calculation approach by Pierre and Murthy [1994]. Schrape et. al. [2006a, 2006b] investigated the effects of in- and also anti-phase-blade-motion of tuned and mistuned blisks on aerodynamical damping.

All of the previous characteristics of mistuned bladed disk have to be regarded during the design and test-phase of future aero engine rotors. In this context, the maximum blade amplitude magnification and the splitting of the double modes play major roles for resonance excitability and high cycle vibration fatigue, whereas mode localization has to be kept in mind for rotor instrumentation. Due to the demand for an acceptable signal-to-noise ratio only blades with high amplitudes are suitable. From this results, that an optimum choice of only a few blades to be instrumented with strain gauges (*s/g*) is the basis of a convincing vibration monitoring systems during rig tests.

Up to now the ability to predict the sensitivity of different blisk designs and blade vibration modes to mode localization and the knowledge how to design less mistuning sensitive blisks is still missing.

To achieve a better understanding of these contexts both the free and the forced vibrational behavior of *HPC*-front rotor stages is analyzed using different evaluation factors.

2. VIBRATIONS OF TUNED BLISKS

2.1 Natural Vibrations

Integrated bladed disks have a multitude of different eigenmodes, which can be characterized by the number of diametric and concentric nodal lines.

In general the eigenmodes of a tuned blisk (with blades, which have the same material and geometry) can be divided up into three categories: disk-dominated, blade-dominated and „coupled“ vibrations.

2.1.1 Disk Vibrations

The disk dominates the vibration mode of the whole blisk. The blades can be idealized as covibrating rigid bodies, which contain only a small part of the total blisk strain energy (see FIG. 3).

Due to the existence of nodal diameters a cyclic symmetry mode (*CSM*) appears. The maximum number of nodal diameters depends on the blade number *N*:

$$CSM_{max} = \frac{N}{2} \text{ for even } N, \quad (1)$$

$$CSM_{max} = \frac{N-1}{2} \text{ for odd } N \text{ respectively.} \quad (2)$$

Caused by the homogeneous mass- and stiffness distribution the eigenmodes of the blisk have no spatial orientation

regarding to the blisk. In the special case of *CSM*-0, also known as umbrella mode, the number of nodal diameters is zero.

2.1.2 Blade Vibrations

Neglecting the three-dimensional geometry of modern compressor blades as a first assumption, the blades can be considered as a plain plate.

Generally the fundamental eigenmodes with the lowest eigenfrequencies of a cantilever plate are the 1st flap- and the 1st torsional mode, respectively. Depending on the aspect ratio of the plates, modes with higher eigenfrequencies will follow, e.g. higher flap- or torsional modes and also other complex blade modes like edge modes, tramline modes e.g. (see FIG. 2).

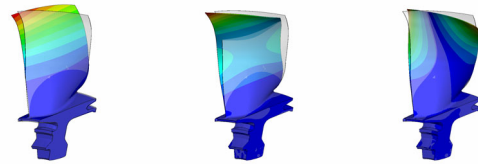


FIG 2. Fundamental blade vibration modes (1st flap mode [left], 2nd flap mode [middle], 1st torsional mode [right], magnitude of displacements), fixed sector model, *Engine-3E-II-HPC* rotor 1

Analogous to the disk-dominated modes, nodal diameters also appear in blade-dominated modes. There are 0 to CSM_{max} characteristic nodal diameters per fundamental blade mode (see Figures 4 and 5). Equations (1) and (2) are valid.

The maximum number of blade vibration modes can be determined to N (CSM_{max} double eigenvalues and one single eigenvalue in case of odd N and $(CSM_{max} - 1)$ double eigenvalues and two single eigenvalues in case of even N respectively¹).

If the system is tuned, all blades have similar displacement amplitudes, which occur with a delay of the inter-blade phase angle:

$$\varphi_{CSM} = \frac{2\pi CSM}{N}, \quad CSM = 0, \dots, CSM_{max}. \quad (3)$$

2.1.3 „Coupled“ Vibrations

The so called „coupled“ vibration modes represent a combination of disk- and blade-modes. Caused by the physical connection between the disk and the blades all vibration modes are coupled, so the notation is not indisputable.

In technical terminology this term is used for vibration modes, where both, disk and blades, store a similar high quantity of the total blisk strain energy (see FIG. 3).

This classification of blisk modes supports the improved rating of *HCF*-sensitive vibration modes because generally only blade modes result in critical strain levels. So a benefit results for strain gauge calibration, where only blade modes have to be included to refer *s/g* response signals to blade displacement amplitudes. If adjacent disk- and/or coupled

1. If $CSM = CSM_{max}$, all blades oscillate in opposite phase to each other.

modes with dominating disk displacements and negligible blade displacements are included, misinterpretations of vibration monitoring system results are probably.

The coupling diagram offers the possibility to illustrate the complex vibrational behavior of a blisk. The eigenfrequencies are printed in dependence on the number of nodal diameters (see FIG. 4).

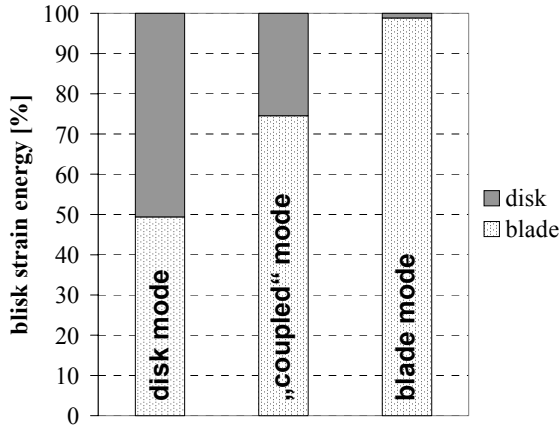


FIG 3. Percentage of blades and disk of whole blisk strain energy (mean value of double eigenmodes), Engine-3E-II-HPC rotor 1

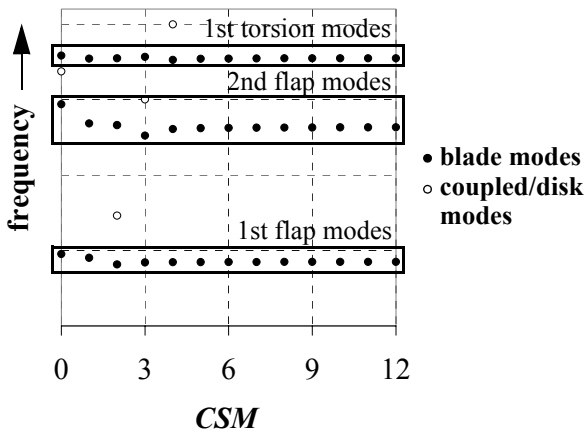


FIG 4. Coupling diagram of Engine-3E-II HPC stage 1, illustration of the 1st three blade modes, free boundary conditions

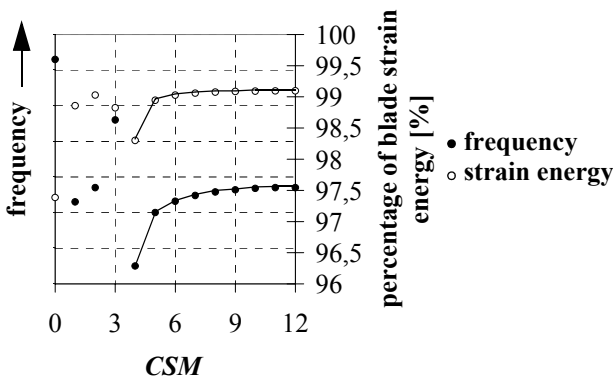


FIG 5. Enlarged section of the coupling diagram compared to the blade percentage on whole blisk strain energy, 1st torsion modes, free boundary conditions, Engine-3E-II-HPC rotor 1

Looking at all modes of one fundamental blade mode family, one can recognize that generally the eigenfrequencies increase up to the frequency of the clamped blade with an ascending number of nodal diameters (see FIG. 5)¹.

The reason for that is the stiffer reaction of the disk with ascending number of nodal diameters (see also Malkin [1942] and Soares [1972]).

In general blade vibration modes govern the maximum operational lifetime of compressor rotors caused by the high strain level of the blades, so the focus of the following chapters is located on these. In this context disk and „coupled“ modes will be neglected for further investigations.

2.2 FORCED VIBRATIONS OF TUNED BLISKS

Especially wakes, generated by circumfluted upstream and downstream located guide vanes as well as blades and their multiples excite corresponding blisk modes at every rotor revolution in operation (see also Yingfeng [2005]). The number of existing wakes determines the value of the engine order (EO).

According to the requirement of congruity of vibration mode shape and excitation mode shape, the k th CSM can only be excited by k th EO respectively k th-aliasing EO. One particular feature of forced responses of a tuned blisk are the similar displacements of all blades, which appear phase-shifted to each other.

3. VIBRATIONS OF MISTUNED BLISKS

If the blade eigenfrequencies f_N differ from each other, caused by different blade geometries due to the manufacturing process (milling, polishing, friction welding, etc.) and material inhomogeneities of the alloy, mistuning of the blisk occurs. The level of mistuning can be assessed using the blade frequency standard deviation ($\sigma_{mistuning}$).

At this point it has to be mentioned that integrated bladed disks are very sensitive already to slight blade mistuning (see also Beirow [2005]).

3.1 Modeling of Blade Mistuning

The modeling of mistuning of the individual blades of the full FE-model can be realized by changing of the material properties: Due to the decrease and increase of the individual blade Young's modulus E_i the blade eigenfrequencies can be modified without changing the blade geometry (*material dependent mistuning*) respectively.

The Young's modulus of the disk is constant. It is valid:

$$f_i \sim \sqrt{E_i}. \quad (4)$$

The change of blade eigenfrequencies is proportional to the change of the square root of the blade Young's moduli.

In contrast to the measured mistuning distributions, which differ for each fundamental blade mode, different sinusoidal blade mistuning deviations exclusively are used to get better clearness comparing different blade modes and mistuning levels with each other (see FIG. 6).

Here, the numbers of full sine waves around the blisk circumference were chosen to 1, 4 and CSM_{max} with standard deviations of 0.07%, 0.15%, 0.24%, 0.68%, 1.36% and 2.71%.

1. Often blisk vibration modes with a low number of nodal diameters are exceptional cases in case of free conditions.

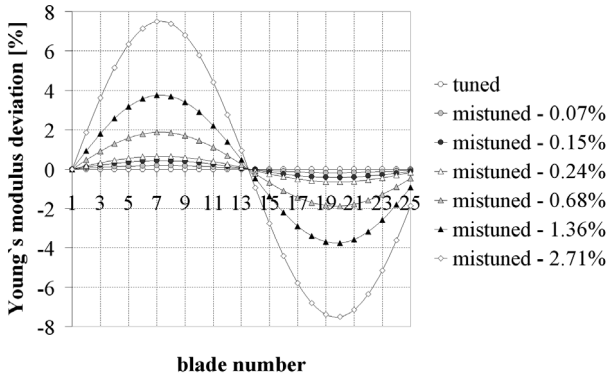


FIG 6. Different artificial sinusoidal mistuning distribution caused by blade Young's modulus modification of Engine-3E-II-HPC rotor 1

3.2 Natural Vibrations of Mistuned Blisks

Generally, the mistuning of a blade-disk-assembly results in several fundamental effects:

3.2.1 Splitting of Double Eigenvalues

The pairwise appearing eigenvalues of the system are split into two closely adjacent eigenvalues caused by the missing symmetry (illustrated by the displaced [low mistuning level] or vanished nodal diameters [higher mistuning level], see also FIG. 8). Generally a stronger mode splitting can be observed with higher eigenfrequencies. The associated double eigenmodes (so called double modes) with different eigenfrequencies have a fixed orientation to the blisk. Increasing the mistuning of the system, the distance between the adjacent eigenfrequencies increases (for further informations see Kellerer [1982]).

3.2.2 Modification of Mode Shapes & Mode Localization

After mistuning, purely sinusoidal vibration modes of the tuned system are transformed into a superposition of many single sinusoidal vibration modes, where the shares of the several harmonics vibrations may be different.

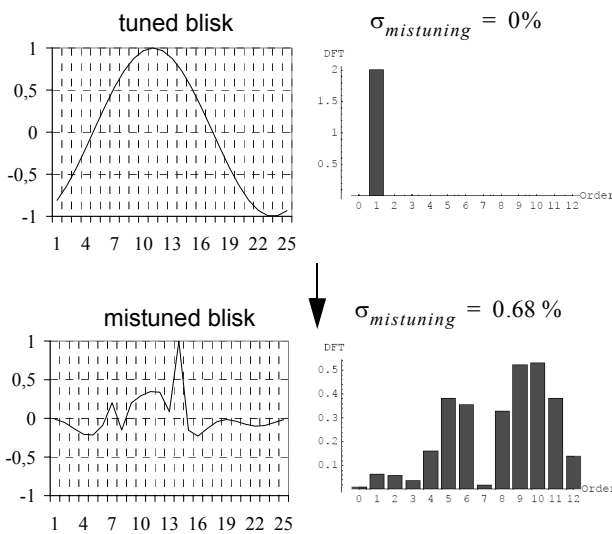


FIG 7. Left: normalized axial displacements at all leading edge tips of (M)CSM 1 (torsion mode); right: Fourier decomposition of the vibration mode

Locally limited and variable blade displacements appear around the blisk's circumference, the so-called mode localization (see FIG. 7). The extreme case is the fully localized mode characterized by only one oscillating blade.

Thus a clear assignment of single vibration modes to a CSM becomes more difficult. So, caused by the displaced nodal diameters the CSM are transformed into Modified Cyclic Symmetry Modes (MCSM) in case of slight mistuning. With increasing mistuning also the warped nodal diameter lines vanish (see FIG. 8).

Mode localization is indicating for the modified vibrational behavior of mistuned blisks.

3.3 Evaluation using the Localization Factor

In case of mistuned blisks it is possible that a number of blades reach high magnification factors and only one single blade reaches a higher displacement level. Because of the need for an optimum choice of blades to be instrumentated this information is highly relevant in terms of s/g application of rotor stages.

In addition of the magnification factor, which includes the maximum displacement magnification regarding the tuned system of all blades in case of forced response, the localization factor, which is introduced below, shows how many blades strongly participate in this mode.

This computational method transforms the complex vibrational behavior of a huge number of blades into one illustrative indicator to ensure an efficient and fast evaluation of the localization sensitivity of different blisk designs and blade modes. A further approach can be found in Kahl [2002].

3.3.1 Tuned Systems

With exception of CSM 0, where all blades have an identical displacement at the same time t , all of the other vibration modes are characterized by discrete sine waves around the circumference depending on the CSM.

A special feature of the undisturbed sine waves is the constant ratio of the maximum blade displacement amplitude $\hat{U}_{i,max}$ to the root mean square of all blade displacement values. So

$$RMS_{U_{i,tuned}} = \sqrt{\frac{1}{N} \sum_{j=1}^N U_{ij}^2}, \quad (5)$$

is independent on the number of sine waves around the circumference (see FIG. 9, left). This should be the basis of the following calculations.

In case of $1 \leq CSM \leq CSM_{max}$ (odd N) and $1 \leq CSM < CSM_{max}$ (even N) the ratio of the maximum blade displacement amplitude to the root mean square of all blade displacements, ζ_{tuned} , is

$$\zeta_{tuned} = \frac{\hat{U}_{i,max}}{RMS_{U_{i,tuned}}} = \frac{\hat{U}_{i,max}}{U_{i,max} \times 1/\sqrt{2}} = \sqrt{2}. \quad (6)$$

In case of the umbrella mode with $\hat{U}_{i1} = \hat{U}_{iN} = \hat{U}_{i,max}$ or CSM_{max} (even N) with $RMS_{U_{i,tuned}} = U_{i,max}$ follows:

$$\zeta_{tuned} = \frac{\hat{U}_{i,max}}{RMS_{U_{i,tuned}}} = \frac{\hat{U}_{i,max}}{U_{i,max} \times 1} = 1. \quad (7)$$

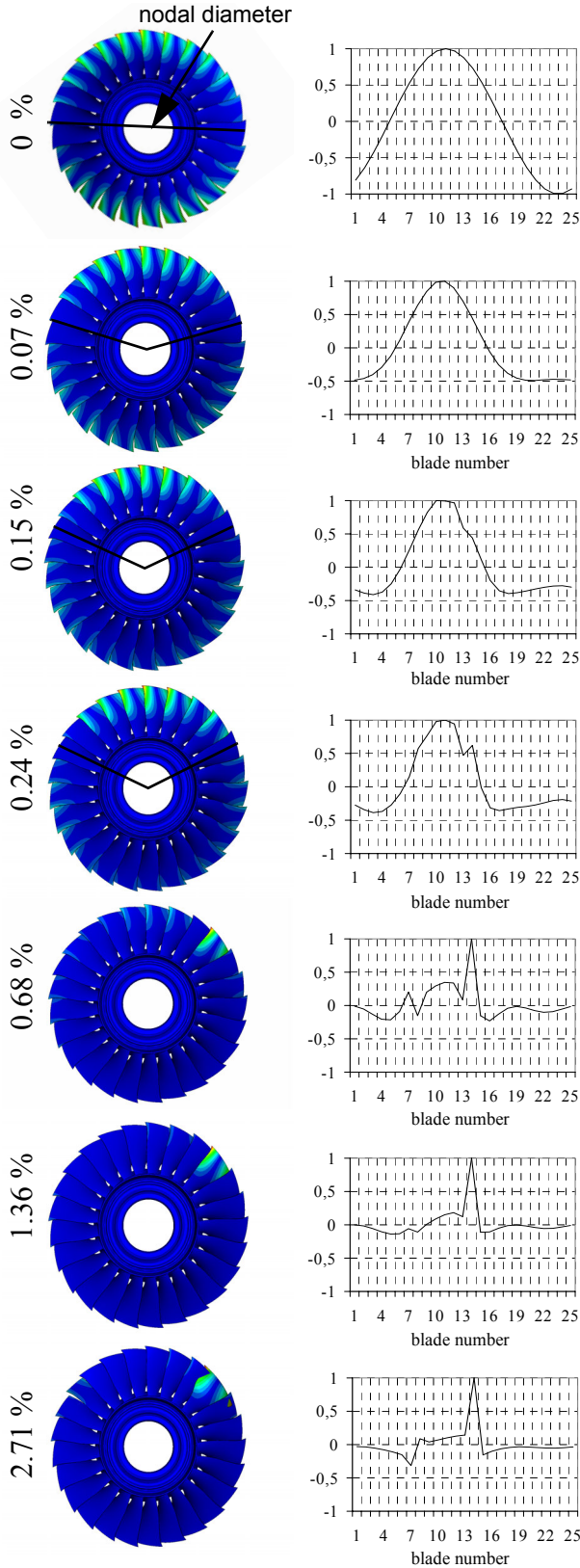


FIG 8. Influence of different blade mistuning levels on vibration modes (1st torsion modes, $(M)CSMs$ 1; left: displacement amplitudes; right: normalized axial displacements of each leading edge blade tips, *Engine-3E-II-HPC* rotor 1

3.3.2 Mistuned Systems

Due to the deviations of the eigenmode of the mistuned system compared to the tuned one, the root mean square of the blade displacements decreases (see FIG. 9, right).

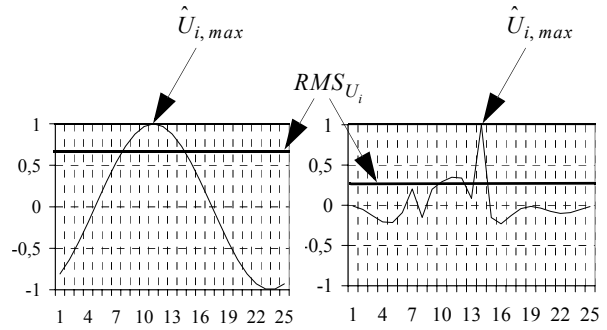


FIG 9. Normalized axial blade displacements at all leading edge tips of *CSM* 1 (left) and *M-CSM* 1 (right), 1st torsion modes

The maximum mode localization, that is characterized by only one oscillating blade, results in the minimum root mean square value:

$$RMS_{U_{i,mistuned,min}} = \sqrt{\frac{1}{N}U_{i,max}^2} = \sqrt{\frac{1}{N}U_{i,max}} \quad (8)$$

The maximum ratio of the maximum blade displacement amplitudes to the root mean square of all blade displacements, $\zeta_{mistuned,max}$, is defined as:

$$\zeta_{mistuned,max} = \frac{\hat{U}_{i,max}}{RMS_{U_{i,mistuned,min}}} = \frac{\hat{U}_{i,max}}{\sqrt{\frac{1}{N}U_{i,max}}} = \sqrt{N} \quad (9)$$

$$\text{for } 0 \leq (M)CSM \leq CSM_{max}$$

and just depending on the number of blades N .

3.3.3 Definition of the Localization Factor

The transformation of the blade number dependent ratio ζ into the localization factor *LocaFac* is necessary for the comparability of the mode localization strength of blisk designs with different blade numbers. This factor describes the local limitation of the vibration mode in a defined range of 0% (no mode localization) up to 100% (maximum mode localization, only one blade oscillating).

Consequently the localization factor is defined as

$$LocaFac = \frac{100}{\sqrt{N}-\sqrt{2}}(\zeta-\sqrt{2}) \text{ [%]} \quad (10)$$

$$\begin{aligned} &\text{if } 1 \leq (M)CSM \leq (M)CSM_{max} \text{ (odd } N) \\ &\text{or } 1 \leq (M)CSM < (M)CSM_{max} \text{ (even } N), \end{aligned}$$

and

$$LocaFac = \frac{100}{\sqrt{N}-1}(\zeta-1) \text{ [%]} \quad (11)$$

$$\begin{aligned} &\text{if } (M)CSM = 0 \\ &\text{or } (M)CSM = (M)CSM_{max} \text{ (even } N) \end{aligned}$$

respectively.

The evaluation criterion of mode localization is exemplarily computed for stage 1 of the *Engine-3E-II-HPC*. Again the measured blade mistuning distribution is substituted by different artificial sinusoidal blade mistuning distributions with different mistuning levels to ensure the comparability of different blade modes and damping conditions.

3.3.4 Influence of Mistuning Level and Blade Mode

Starting from the tuned system without any mode localization, a continuous rise of the localization factors can be observed with increasing blade mistuning for all of the three fundamental blade modes as well as the disk and „coupled“ modes (see FIG. 10).

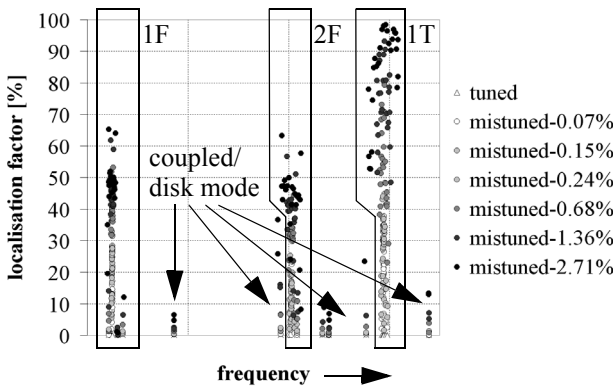


FIG 10. Localization factors of natural vibrations depending on the blade mistuning standard deviation (first three blade modes) 1-sine-wave mistuning distribution around blisk circumference

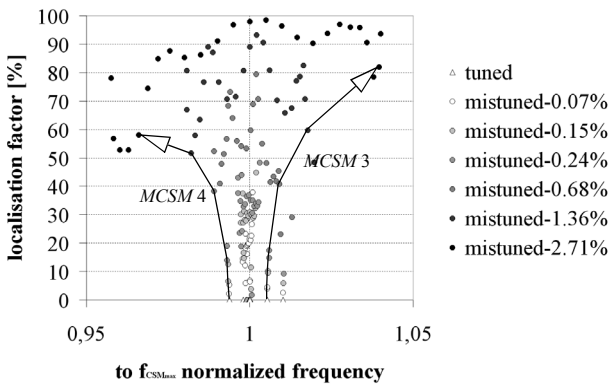


FIG 11. Localization factors of natural vibrations depending on the blade mistuning standard deviation of 1st torsion modes 1-sine-wave mistuning distribution around blisk circumference

The maximum mode localization independently appears from the mistuning level for the highest cyclic symmetry mode MCSM 12 (maximum $LocaFa \approx 98.4\%$ at $\sigma_{mistuning} = 2.71\%$) in case of 1-sine-wave-blade-mistuning distribution (see FIG. 11).

It has to be mentioned, that in case of lower MCSM ($1 \div 4$) significant lower localization factors occur.

At this point it can be also recognized that disk and „coupled“ modes are less sensitive to mode localization due to their lower blade percentage on the whole blisk strain energy (see Figures 10 and 12). In contrast to the medium localization factors of mistuned flap modes, the mode localization of torsion modes is more pronounced caused by the lower coupling between the individual blades (see Figures 11 and 12). Furthermore the bandwidth of eigenfrequencies increases with rising mistuning levels - the eigenfrequencies of the various vibration modes are bearing off from each other (see FIG. 11), so the bandwidth of

possible blade mode resonances enlarges, which has to be regarded to avoid critical resonances in operation during the aero engine development.

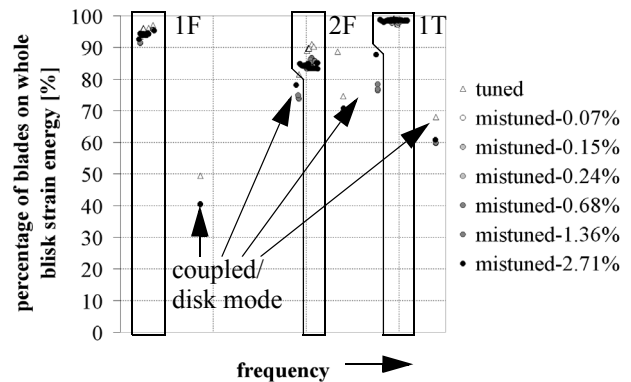


FIG 12. Percentage of blades on whole blisk strain energy of natural vibrations depending on the blade mistuning standard deviation (first three blade modes), 1-sine-wave mistuning distribution around blisk circumference

With an increased mistuning level the percentage of blades on the whole blisk strain energy decreases due to lower number of mode-participating blades. So, in case of the high localized torsion modes the mean value of blade share decreases from 98.8% to 98.4% (in addition: 1st flap mode: 95.9% \rightarrow 93.9%, 2nd flap mode: 89.1% \rightarrow 83.5%, see Figures 12 and 13).

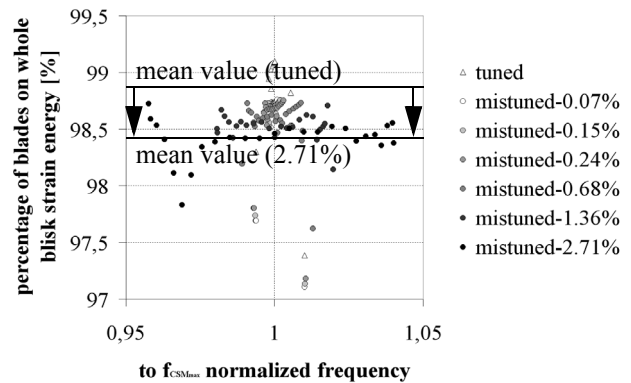


FIG 13. Percentage of blades on whole blisk strain energy of natural vibrations depending on the blade mistuning standard deviation of 1st torsion mode, 1-sine-wave mistuning distribution around blisk circumference

The mean localization factors of all three sinusoidal blade mistuning distributions of the first three fundamental blade modes are presented in dependence on from the mistuning standard deviation in Figure 14.

As one can recognize, the curve shapes of the localization factors are very sensitive regarding blade mistuning for small mistuning levels ($0\% < \sigma_{mistuning} \leq 0.2\%$). A nearly linear context between mistuning standard deviation and localization factor occurs. With increasing mistuning standard deviations local maxima and minima can appear ($0.2\% < \sigma_{mistuning} \leq 0.4\%$) followed by a continuously rise

of the localization factors ($\sigma_{mistuning} < 0.4\%$) up to 67.5% (1st flap mode), 68.3% (2nd flap mode) and 97.5% (1st torsion mode).

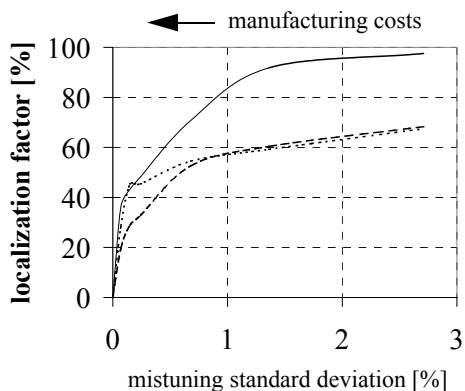


FIG 14. Maximum localization factors of first three blade modes depending on the blade mistuning standard deviation; ... 1st flap mode, --- 2nd flap mode, — 1st torsion mode, averaging of three artificial sine blade mistuning distributions

3.3.5 Effect of Disk Stiffness

Because of the known influence of disk stiffness on inter-blade coupling (see R. Bladh [2003] and S. Baik [2004]), aero engine manufacturers are interested in reducing mode localization as well as amplitude magnification using modified hub sections to extend service life.

To verify suitable disk stiffness ratios, the Young's modulus of the disk section was modified about $\pm 50\%$ of the original value.

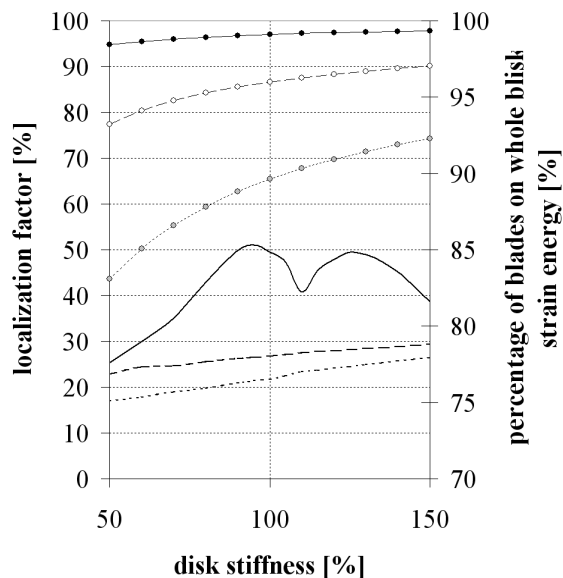


FIG 15. Percentage of blades on whole blisk strain energy ($\circ \circ \bullet$) compared to the resulting averaged localization factor of natural vibrations depending on the disk stiffness; ... 1st flap mode, --- 2nd flap mode, — 1st torsion mode, averaging of three artificial sine mistuning distributions

As presented in figure 15 the percentage of blades on the whole blisk strain energy steadily increases with higher disk

stiffness, because of a stiffer embedding of the blades on the disk.

As a result the eigenfrequencies of the blade modes as well as the eigenfrequencies of the disk and „coupled“ modes become higher.

In case of the first and second blade flap mode the decreased inter-blade coupling, that corresponds with the percentage of the blades on the whole blisk strain energy, results in higher localization factors. In contrast to this, in case of the first blade torsion modes local maxima (at 95% and 125% of the original disk stiffness) and minima (at 70% and 115% of the original disk stiffness) occur.

Aiming at a minimization of the mode localization effects, the modification of the disk stiffness has to regard all of the relevant blade modes. Within the realms of constructive possibilities and without consideration of local maxima and minima this means a reduction of disk stiffness to increase the inter-blade coupling and to decrease the structural blade-to-blade isolation.

3.4 Forced Vibrations of Mistuned Blisks

At the current state of the art a completely symmetric manufactured, tuned blisk without any imperfections is not possible. Thus, a mistuned, excited blisk can be treated as a rule during operation of an aero engine.

During both, operation and rig test runs aerodynamical forces excite compressor rotors in dependence on from its operating point. Aerodynamic damping¹ including fluid-structure-interactions² and structural damping³ limit the resulting blade amplitudes. At this a modal damping value of $D=0.1\%$ ($Q=500$) was selected as basis of the following analyses. Engine orders 1, 4 and CSM_{max} were chosen for the illustration of various forced responses.

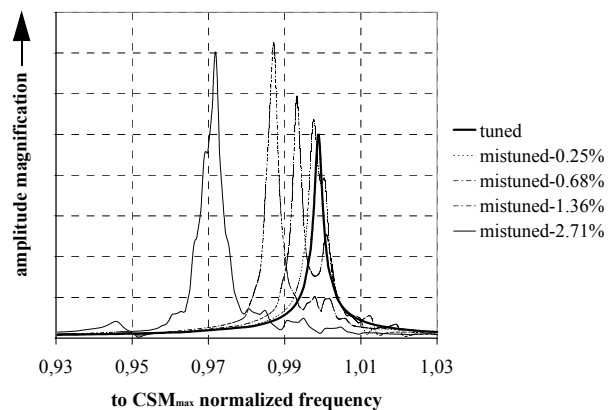


FIG 16. FRFs of blade # 6 for different mistuning levels, EO 1, 1st torsion mode, magnitude amplification of axial displacements of leading edge blade tips, $D=0,1\%$ ($Q=500$)

Induced by the huge number of different Fourier coefficients of the modified vibration modes, many resonance peaks

1. caused by the airflow around the blades
2. Anti-phase-blade-vibrations of tuned and mistuned bladed disks result in additional aerodynamic forces and aerodynamic damping due to the compression of the flow between the vibrating blades. For further informations see also Schrape [2006a, 2006b].
3. Only the material damping occurs because of the missing blade-disk-connection of blisks.

can be observed in the frequency response function (*FRF*) of the individual blades due to excitation of the *k*th engine order. Each peak correlates with a vibration mode, which has also a *k*th harmonic in its Fourier decomposition. The maximum amplitude level of the *FRF* depends on the percentage of the *k*th harmonic on all Fourier coefficients (see FIG. 16). See also Mück [2004], Pianka [2004], Wei [1987a, 1987b].

3.5 Influence of Mistuning Level and Blade Mode

Using the three artificial sinusoidal blade mistuning distributions with different standard deviations in combination with *EO* 1, 4 and CSM_{max} a non-linear context between localization factor, amplitude magnification and the level of mistuning was determined (see Figures 17 and 18).

The curve shapes of the forced response results resemble the curve shapes of the former determined eigenmodes (see FIG. 14). Again localization factors of the torsion modes are higher than corresponding values of the 1st and 2nd flap modes at identical mistuning levels. As maximum localization factors 83.0 % for 1st torsion mode, 70.3 % for 1st flap mode and 61.4 % for 2nd flap mode are found.

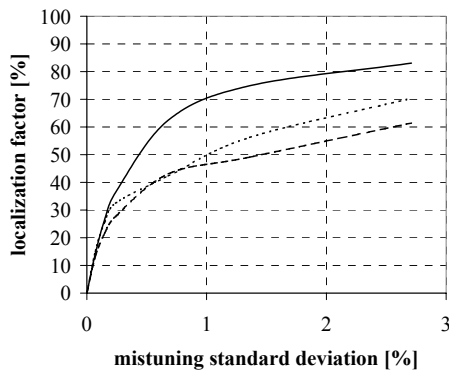


FIG 17. Maximum localization factor of forced response depending on the first three blade modes; ... 1st flap mode, --- 2nd flap mode, — 1st torsion mode, $D=0.1\%$ ($Q=500$), averaging of *EOs* 1, 4, 12 (CSM_{max}) and three artificial sine mistuning distributions

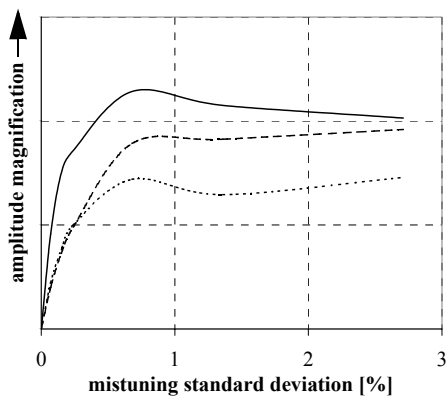


FIG 18. Maximum amplitude magnification of forced response depending on the first three blade modes; ... 1st flap mode, --- 2nd flap mode, — 1st torsion mode, $D=0.1\%$ ($Q=500$), averaging of *EOs* 1, 4, 12 (CSM_{max}) and three artificial sine mistuning distributions

At this point the selected medium modal damping value of $D=0.1\%$ reduces the markedness of the local maxima and minima compared to the eigenmode analysis (see also chapter 3.5.1 “Effect of Modal Damping”).

Because of the non-symmetric mode shapes in case of mistuned blisks the individual amplitudes differ from blade to blade. This results in amplitude magnifications for some blades and also in a minification of amplitudes for other blades. Figure 18 presents the averaged maximum blade amplitude magnification for *EO* 1, 4 and CSM_{max} of the three fundamental blade modes.

In case of the 1st torsion mode and the 1st flap mode the maximum amplitude magnifications occur at the local maxima at $\sigma_{mistuning} \approx 0.8\%$, while the absolute maximum of the 2nd flap mode occurs at $\sigma_{mistuning} = 2.71\%$. Over-all, due to the lower interblade-coupling and the resulting higher structural isolation forced torsion modes are more sensitive regarding blade mistuning than flap modes.

It can be summarized that generally mode localizations steadily increases with higher mistuning levels, while the maximum displacement amplitude magnification of a slightly mistuned system appears at moderate mistuning standard deviations.

3.5.1 Effect of Modal Damping

Figure 19 exemplarily presents the context between *FRFs* of blade # 6 and normalized excitation frequency in case of *EO* 1 in dependence on the modal damping value.

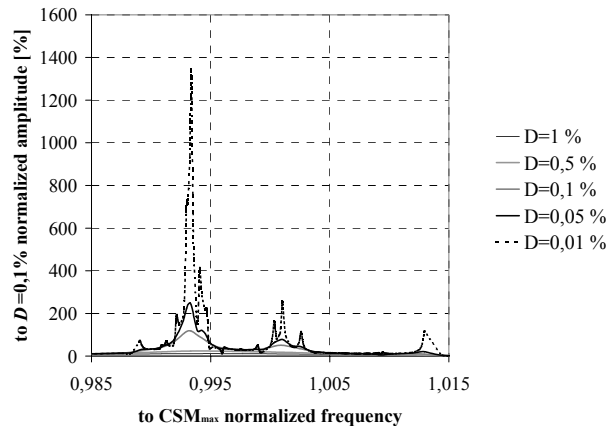


FIG 19. *FRFs* of blade #6 depending on the damping value, forced response analysis for *EO* 1, $\sigma_{mistuning} = 0.68\%$, 1 sine-wave mistuning, 1st torsion mode

As one can discern, each eigenmode, which includes an appropriate coefficient in their Fourier decomposition, undergoes a mode localization during excitation. Not only the resonance peaks decrease with increased damping, but also adjacent resonance peaks merge in a single wider peak.

This results in decreasing localization factors (see FIG. 20), less pronounced local minima and maxima of amplitude magnification and reduction of the maximum blade displacements (see FIG. 21).

So, high modal damping is the advantageous regarding mode localization and amplitude magnification. This means operational conditions with high aerodynamic damping rather result in lower localized blade mode shapes than condi-

tions with low aerodynamic damping.

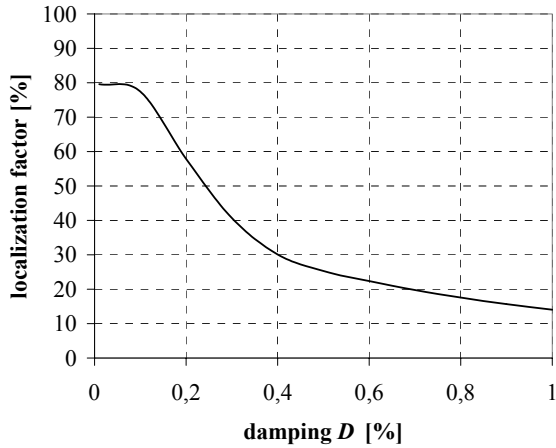


FIG 20. Maximum localization factor depending on the damping value, forced response analysis for EO 1, $\sigma_{mistuning} = 0.68\%$, 1 sine-wave mistuning, 1st torsion mode

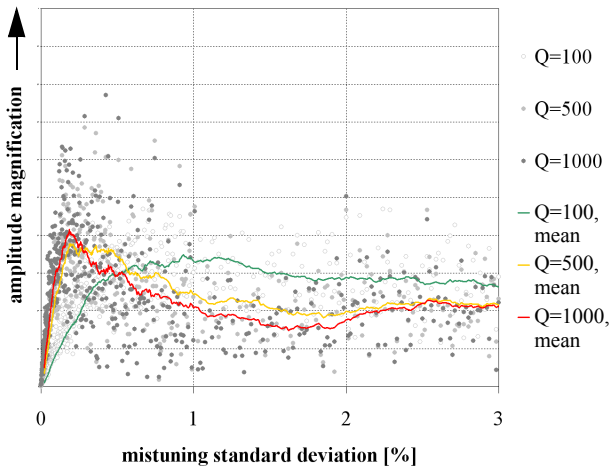


FIG 21. Maximum blade displacement magnification depending on the damping value and mistuning standard deviation, forced response analysis for EO 8, probabilistic mistuning samples, 1st flap mode, *Engine-3E-I-HPC* rotor 1

3.5.2 Influence of Exciting Engine Order

The probabilistic studies (see FIG. 21) were extended to all engine orders between 0 and CSM_{max} to determine the effects of different EO s. Exemplarily the results for 1st flap mode are shown in Figure 22.

It can be discerned that the maximum blade displacement appear at low EO excitation. Contrary to this a steady reduction of amplitude magnification occur up to $EO \approx 0.7 \times CSM_{max}$. For higher EO s blade amplitudes increases again (see FIG. 23).

At this local maxima resulting from low EO excitations occur at higher mistuning levels compared to higher EO excitations, which cause maximum amplitude magnifications at lower mistuning levels.

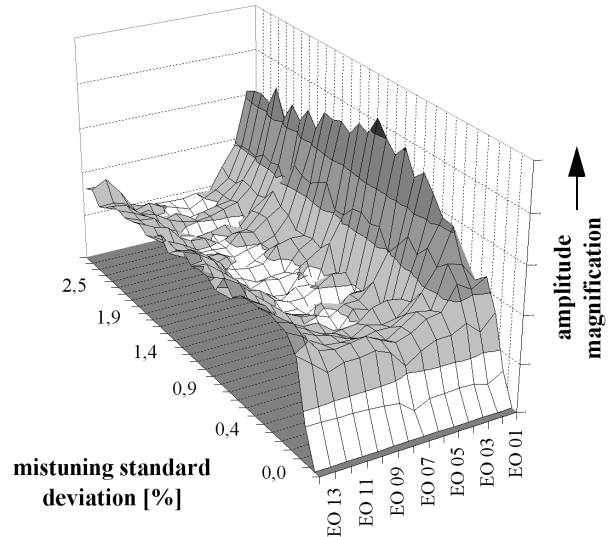


FIG 22. Averaged amplitude magnifications of 1st flap modes depending on the EO excitation and the mistuning level, forced response analysis, $D=0.1\%$ ($Q=500$), *Engine-3E-I-HPC* rotor 1

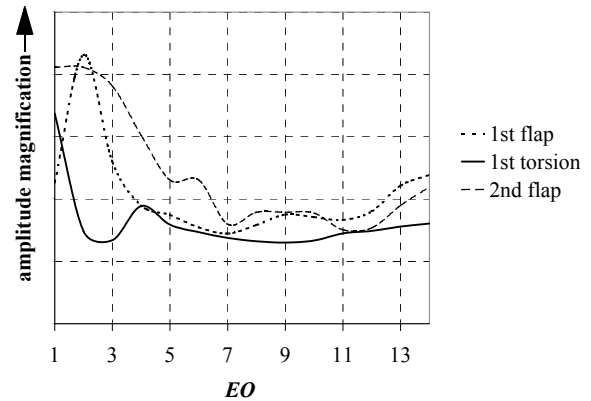


FIG 23. Maximum amplitude magnifications of first three blade modes depending on the EO excitation, *Engine-3E-I-HPC* rotor 1, $D=0.1\%$ ($Q=500$)

4. CONCLUSIONS & SUMMARY

Due to the very low structural damping the appearing vibration modes of blade integrated disks (blisks) are very sensitive to individual blade mistuning. In contrast to the tuned design model, characterized by similar blade amplitudes for all blades, a more or less local zoning of the vibration modes occurs, the so called mode localization.

For a clear and objective comparison of various blisk designs and excitation parameters the *localization factor* have been introduced.

Front *HPC* rotors of the German *Engine 3E* research program has been used for the comparison of the vibrational behavior of different mode shapes, damping values and disk stiffness ratios.

The determined localization factors and amplitude magnifications show, that in general torsion modes of mistuned blisks have a more pronounced local zoning of vibration modes than flap modes. These higher sensitivity regarding blade mistuning, results from a stronger structural isolation of the adjacent individual blades due to their lower inter-

blade coupling, which can be characterized using the percentage of blades or disk resp. on the whole blisk strain energy.

The same effect is valid for non-cyclic-symmetric blade modes, that arose from cyclic symmetry modes caused by blade mistuning: Modes with lower numbers of (warped) nodal diameter lines are less sensitive regarding mistuning than blade modes, that arose of modes with larger numbers of nodal diameter lines. The different inter-blade coupling of these blade modes is the causal of this effect.

Generally a decline of mode localization can be observed, if a disk stiffness is decreased due to design modifications. Depending on the blisk geometry a slight increase of all absolute blade displacement amplitudes occurs, caused by the softer fixation of the blades on the disk.

In general, maximum amplitude magnifications of forced vibrations appear at moderate mistuning levels for slightly tuned systems, while the localization of blade modes steadily increases with higher blade mistuning.

The knowledge of these connections are used for the improvement of future blisk design (sensitivity to mode localization, design and/or modification of hub section), the prediction of maximum blade loads in operation and also the instrumentation of blisk using strain gauges, especially the determination of suitable blades for strain gauge instrumentation during rig tests (see also Klauke [2005]).

ACKNOWLEDGMENTS

The work presented in this paper has been supported by Rolls Royce Deutschland GmbH & Co KG. The authors thank for this commitment. The investigations are part of the DeSK blisk validation program (FKZ: 80121978), which is funded by the state of Brandenburg and the European Fund for Regional Development (efreinfo@mw.brandenburg.de).

REFERENCES

Armstrong, E. K., 1955, „An Investigation Into The Coupling Between Turbine Disc And Blade Vibration“, Ph. D. Thesis, University of Cambridge

Baik, S., Pierre, C., Castanier, M.P., 2004, „Mistuning Sensitivity Prediction of Bladed Disks Using Eigenvalue Curve Veerings“, Proceedings of the 9th National Turbine Engine HCF Conference, Pinehurst, NC, U.S.A.

Beirow, B., Kühhorn, A., Golze, M., Klauke, T., Parchem, R., 2005, „Experimental and Numerical Investigations of High Pressure Compressor Blades Vibrational behaviour Considering Mistuning“, 10th International NAFEMS World Congress, Malta, ISBN 1 174 376 03 4

Bladh, R., Pierre, C., Castanier, M.P., 2003, „Effect of Multistage Coupling Disk Flexibility on Mistuned Bladed Disk Dynamics“, ASME Journal of Engineering for Gas Turbines and Power, Vol. 125, pp. 121-130

Campbell, W., 1924, „The Protection Of Steam Turbine Disk Wheels From Axial Vibration“, ASME, 46, No. 1920, pp. 31-160

Dello, J., 1987, „Frequency Evaluation Of A Steam Turbine Bladed Disk“, Dresser-Rand, Wellsville, NY, U.S.A.

Ewins, D. J., 1969, „The Effects Of Detuning Upon The Forced Vibrations Of Bladed Disks“, Journal of Sound and Vibration, Vol. 9, No. 1, pp. 65-79

Ewins, D. J., 1973, „Vibration Characteristics of Bladed Disc Assemblies“, J. Mech. En. Sci. 15, pp. 165-186

Griffin, J.H., Hoosac, T.M., 1984, „Model Development and Statistical Investigation of Turbine Blade Mistuning“, ASME Journal of Vib., Acoust., Stess, Rel. Des., Trans., No. 106 (2), pp. 204-210

Imregun, M., 1999, „Structural Dynamics: Basics Of Disk And Blade Vibration“, Imperial College, Mechanical Engineering Department, London

Kahl, G., 2002, „Aeroelastic Effect of Mistuning and Coupling in Turbomachinery Bladings“, Ph.D. thesis, Ecole Polytechnique Federale De Lausanne, These-No. 2629

Kellerer, R.; Stetter, H., 1992, „Double Mode Behaviour of Bladed Disk Assemblies in the Resonance Frequency Range, Visualized by Means of Holographic Interferometry“, ASME 92-GT-438, also presented at the International Gas Turbine and Aeroengine Congress and Exposition, Cologne, Germany, 1992, (Z 457)

Kielb, R.E., Kaza, K.R.V., 1984, „Effects of Structural Coupling on Mistuned Cascade Flutter and Response“, ASME Journal of Engineering for Gas Turbines and Power, Vol. 106, pp. 17-24

Kirkhope, J.; Wilson, G. J., 1971, „Analysis Of Coupled Blade Disk Assemblies In Axial Flow Turbine And Fans“, Proc. 12th AIAA/ASME Structures, Structural Dynamics and Material Conference, AIAA Paper No. 71-375, pp. 1-11

Klauke, T., Kühhorn, A., Beirow, B., 2005, „Experimental and Numerical Investigations of Blade Mistuning and Strain Gauge Application Effects in Aero Engine Development“, 12th Blade Mechanics Seminar, ABB Turbo Systems Ltd., Thermal Machinery Laboratory, Baden/Switzerland

Malkin, I., 1942, „On A Generalization of Kirchhoff's Theory Of Transversal Plate Vibration Problem Of Steam Turbine Disks“, J. Franklin Institute 234, p. 355-370, pp. 431-452

Mück, B., 2004, „Flutter And Forced Response Prediction In Compressor Blade Design“, XI. Blade Mechanics Seminar, Switzerland

Pianka, C., 2004, „Considering Mistuning Effects On Blisks In The Specification Of Engine Vibration Surveys“, XI. Blade Mechanics Seminar, Switzerland

Pierre, C., Murthy, D., 1994, „Localization of aeroelastic modes in mistuned high-energy turbines“, Journal of Propulsion Power, No. 10, pp. 318-328

Schraper, S., Kühhorn, A., Golze, M., 2006a, „Simulation of fluid damped structural vibrations“, Proceedings of the 7th MpCCI User Forum, February 21-22, Schloss Birlinghoven,

Sankt Augustin, Germany, ISSN 1860-6296, 2006

Schrage, S., Kühhorn, A., Golze, M., 2006b, „FSI of a Simplified Aero Engine Compressor Cascade Configuration“, PAMM-Proceedings in Applied Mathematics and Mechanics 6, 457 - 458 (2006) / DOI 10.1002/pamm.200610209

Sever, I. A., 2004, „Experimental Validation Of Turbomachinery Blade Vibration Predictions“, Imperial College London, Department of Mechanical Engineering

Soares, C. A. M.; Petyt, M.; Salama, A. M., 1976, „Finite Element Analysis Of Bladed Disks, Proc. Winter Annual Meeting ASME, pp. 73-92

Steffens, K., 2000, „Next Engine Generation: Materials, Surface Technology, Manufacturing Processes, What comes after 2000?“, SurTec Conference, Cannes, France

Steffens, K., 2001, „Advanced Compressor Technology - Key Success Factor for Competitiveness in Modern Aero Engines“, 15th International Symposium on Air Breathing Engines, ISABE, Bagalore, India

Wei, S. T.; Pierre, C., 1987a, „Localization Phenomena In Mistuned Assemblies With Cyclic Symmetry, Part I: Free Vibrations“, Department of Mechanical Engineering and Applied Mechanics, University of Michigan, Ann Arbor, MI, U.S.A.

Wei, S. T.; Pierre, C., 1987b, „Localization Phenomena In Mistuned Assemblies With Cyclic Symmetry, Part II: Forced Vibrations“, Department of Mechanical Engineering and Applied Mechanics, University of Michigan, Ann Arbor, MI, U.S.A.

Whitehead, D.S., 1966, „Effect of Mistuning on the Vibration of Turbomachine Blades Induced by Wakes“, ASME Journal of Mechanical Engineering and Science, Vol. 8, No. 1, pp. 15-21

Whitehead, D.S., 1998, „The Maximum Factor by Which Forced Vibration of Blades Can Increase due to Mistuning“, ASME Journal of Engineering for Gas Turbines and Power, Vol. 120, pp. 115-119

Wildheim, J., 1979, „Excitation of Rotationally Periodic Structures“, ASME Journal of Applied Mechanics, 46, pp. 878-882

Wilson, A.; Utengen, T., 1993, „Turbine Blade Dynamics And Blade-Vane Interaction In A Radial Inflow Turbine“, Ulstein Turbine A/S, Kongsberg, Norway

Yingfeng, W.; Jun, H.; Yong, Z., 2005, „Effect Of Upstream Rotor On The Aerodynamic Force Of Downstream Stator Blades“, ISABE-2005-1268, Najing University of Aeronautics and Astronautics, China